

**Spectral behavior of the electronic states of bilayer cuprate systems using a slave fermion approach**

Govind,\* Ratan Lal, and S. K. Joshi

*Theory Group, National Physical Laboratory, Dr. K. S. Krishnan Road, New Delhi 110 012, India*

(Received 13 June 2003; revised manuscript received 18 September 2003; published 30 March 2004)

The spectral function for electrons in the normal state of a bilayer cuprate is calculated by employing a slave fermion approach. The electron correlations in the  $\text{CuO}_2$  layers in these cuprates are described by a  $t$ - $J$  model, and the electronic coupling between the two  $\text{CuO}_2$  layers within the same unit cell is introduced via a hopping matrix element ( $t_{\perp}$ ) and an exchange interaction ( $J_{\perp}$ ). The spectral function is calculated for different values of the hole concentration, temperature, and anisotropy at various values of the momentum ( $k_x, k_y$ ). It is found that the bilayer coupling ( $t_{\perp}$ ) significantly affects the behavior of the spectral function. The spectral function around the momentum value  $(\pi, 0)$  for a coupled bilayer cuprate shows a peak much sharper than that for a system of uncoupled layers. Our calculation also suggests a splitting of electronic states of the bilayer cuprates along the  $(\pi, 0)$  direction for the heavily overdoped regime. Calculations of the imaginary part of the self-energy  $\Sigma''_1(k, \omega)$  for a bilayer system have also been presented. It is found that  $\Sigma''_1(k, \omega)$  depends strongly on the momentum and shows a  $\omega^{\alpha}$  dependence on energy with  $1.2 < \alpha < 1.5$  for values of the parameters  $t$  and  $J$  considered in the present calculations.

DOI: 10.1103/PhysRevB.69.094522

PACS number(s): 74.72.-h, 74.25.Jb

**I. INTRODUCTION**

The cuprates such as  $\text{La}_{2-x}\text{Sr}_x\text{CuO}_4$ ,  $\text{YBa}_2\text{Cu}_3\text{O}_{7-\delta}$ , and  $\text{Bi}_2\text{Sr}_2\text{CaCu}_2\text{O}_{8+\delta}$  continue to pose a challenge to our understanding of the dynamics of electrons despite an enormous research effort devoted to them. It has not yet been possible to have a reasonably consistent picture of the electronic excitations in these systems.<sup>1-4</sup> The main interactions which should be considered for a description of the cuprates are (1) the Coulomb interaction among the doped holes and (2) the interaction of doped holes with the antiferromagnetic (AFM) background created by holes of the  $\text{Cu}^{++}$  ions. Treating both of these interactions simultaneously is a formidably difficult task.

On the experimental side, angle-resolved photoemission spectroscopy (ARPES) has been extensively used by a number of workers<sup>5-20</sup> to obtain information about the electronic structure in normal as well as superconducting states of various cuprates. ARPES measurements have been made for single layer cuprates,<sup>5-10</sup> bilayer cuprates,<sup>5,8,11-19</sup> and for trilayer cuprates.<sup>20</sup> ARPES measurement carried out by Ino *et al.*<sup>10</sup> for the single layer  $\text{La}_{2-x}\text{Sr}_x\text{CuO}_4$  system have yielded information about the doping dependence of the spectral function at the  $\mathbf{k}=(\pi, 0)$  and  $(\pi/2, \pi/2)$  points. They have observed that the spectral function at  $\mathbf{k}=(\pi, 0)$  shows a relatively sharp peak just below the Fermi energy at the optimum doping ( $x=0.15$ ) while for the underdoped system ( $x=0.07$ ) the peak is broadened and shifted towards lower energy values. Earlier, Shen and Schrieffer<sup>19</sup> have studied the underdoped bilayer  $\text{Bi}_2\text{Sr}_2\text{CaCu}_2\text{O}_{8+x}$  system. They have found a sharp quasiparticle peak near  $(\pi/2, \pi/2)$  and a broad peak near the  $(\pi, 0)$  direction at low doping. Moreover, they found that upon increasing the hole doping from the underdoped to the overdoped side, the quasiparticle peak about the  $(\pi, 0)$  point becomes sharp and moves towards the Fermi energy.

There have been numerous attempts to calculate the spectral function  $A(\mathbf{k}, \omega)$  in cuprates. The main methods which

are utilized in these studies are exact the diagonalization method,<sup>21-23</sup> the quantum Monte Carlo method,<sup>24-26</sup> the density-matrix renormalization group method,<sup>27,28</sup> and the finite temperature Lanczos method (FTLM).<sup>4,29,30</sup>

In the present paper we investigate the electronic behavior of the normal state spectral function of cuprates for single layer cuprates (such as  $\text{La}_{2-x}\text{Sr}_x\text{CuO}_4$ ) as well as for bilayer cuprates (such as  $\text{YBa}_2\text{Cu}_3\text{O}_{6+\delta}$ ,  $\text{Bi}_2\text{Sr}_2\text{CaCu}_2\text{O}_{8+\delta}$ ) for various doping concentrations. Compared to the large number of theoretical studies for the single layer cuprates,<sup>4,8,21-31</sup> there are only a few theoretical studies for bilayer cuprates.<sup>32-35</sup> To study the normal state of cuprates system we have used the slave-fermion approach.<sup>36,37</sup> For high- $T_c$  cuprates the slave fermion approach was applied by Arovas and Auerbach.<sup>38</sup> These authors restricted their study to the half-filled Hubbard band only. Later, Kane, Lee, and Read<sup>37</sup> employed the slave fermion approach for the study of a single hole present in the AFM state of cuprates. We have used here the slave fermion approach for finite doping and applied the saddle-point approximation through which infinitely large correlations are replaced by local constraints. We have presented results for the hole spectral function  $A(\mathbf{k}, \omega)$ , the imaginary part of the self-energy of holes, density of states, and the hole density. The details of the theoretical formulations are described in Sec. II. We discuss numerical calculations for spectral function and self-energy in Sec. III. In Sec. IV we present our conclusions.

**II. THEORETICAL FORMULATION**

The high- $T_c$  cuprates are strongly correlated systems. In the strong correlation case the on-site Coulomb interaction is much larger than the hopping integral so that the double occupancy of a site is prohibited. In this strong correlation case we can use the  $t$ - $J$  model.<sup>36</sup> We consider bilayer cuprates, such as  $\text{YBa}_2\text{Cu}_3\text{O}_{7-\delta}$  and  $\text{Bi}_2\text{Sr}_2\text{CaCu}_2\text{O}_{8+\delta}$ , where there are two  $\text{CuO}_2$  layers per unit cell. It is well known that in a bilayer system two  $\text{CuO}_2$  layers (of the same

unit cell) are relatively closer ( $\sim 0.4$  nm) to each other than the  $\text{CuO}_2$  layers of a single layer system ( $\sim 1.1$  nm). Hence the coupling between the two layers within the same unit cell of a bilayer system is expected to be much more important compared to coupling between layers of two neighboring unit cells. We therefore have taken into consideration the coupling between two layers in the same cell. We have described each of the individual layers by a  $t$ - $J$  model and the two layers within a cell are coupled via hopping of holes from one layer to another as well as via an exchange coupling between the Cu sites of these two layers. A bilayer cuprate with these couplings between the two copper-oxygen layers can be represented by the following Hamiltonian.:

$$H = - \sum_{i \neq j, l, l'} L_{ll'} \sum_{\sigma} \left\{ t_{ll'} b_{i\sigma l}^+ b_{j\sigma l'} + J_{ll'} S_{il} S_{jl'} - \frac{1}{4} \sum_{\sigma\tau} J_{ll'} b_{i\sigma l}^+ b_{i\sigma l} b_{j\tau l'}^+ b_{j\tau l'} \right\}, \quad (1)$$

where  $L_{ll'} = (1 + \delta_{ll'})/2$ , and

$$t_{ll'} = t_{\parallel} \delta_{ll'} + t_{\perp} (1 - \delta_{ll'}) \quad (2)$$

is the hopping matrix element between the layers  $l$  and  $l'$  {when  $l=l'$  (intralayer) and when  $l \neq l'$  (intrabilayer)}, and

$$J_{ll'} = J_{\parallel} \delta_{ll'} + J_{\perp} (1 - \delta_{ll'}) \quad (3)$$

is the exchange coupling strength between the nearest-neighbor spins. Here interactions are between the electrons of layers  $l$  and  $l'$  ( $l=l'$  in the same  $\text{CuO}_2$  plane and  $l \neq l'$  for different  $\text{CuO}_2$  planes in the same cell). Notice that  $l, l' = 1$  and 2. For clarity, we shall also use  $t_{\parallel}$  for  $t_{11} = t_{22}$ ,  $t_{\perp}$  for  $t_{12} = t_{21}$ ,  $J_{\parallel}$  for  $J_{11} = J_{22}$  and  $J_{\perp}$  for  $J_{12} = J_{21}$ .

The correlated operators  $b_{i\sigma l}^+$  and  $b_{i\sigma l}$  are related to the uncorrelated operators  $c_{i\sigma l}^+$  and  $c_{i\sigma l}$  by

$$b_{i\sigma l}^+ = c_{i\sigma l}^+ (1 - n_{i-\sigma l}), \quad b_{i\sigma l} = (1 - n_{i-\sigma l}) c_{i\sigma l}, \quad (4)$$

where  $n_{i-\sigma l}$  corresponds to the number operator. The spin operators in Eq. (1) are defined as

$$S_{il}^+ = b_{i\downarrow l}^+ b_{i\uparrow l}, \quad (5a)$$

$$S_{il}^- = b_{i\downarrow l} b_{i\uparrow l}^+, \quad (5b)$$

$$S_{il}^z = \sum_{\sigma} n_{i\sigma l} (1 - n_{i-\sigma l}). \quad (5c)$$

According to the slave-fermion approach a single fermion operator can be written as a product of operators representing a spinless charge and a chargeless spin. The constraint condition for these operators on each site is that the number of spinless charges plus the number of spins should be equal to unity. In order to preserve the fermion commutations rules, one of these two operator must obey Bose statistics and the other must obey Fermi statistics. In this paper we represent the spins by boson operators and charge by fermion operators. We therefore express the electron operators in the slave fermion (Schwinger boson) representation. Let  $f_{il}^+$  ( $f_{il}$ ) de-

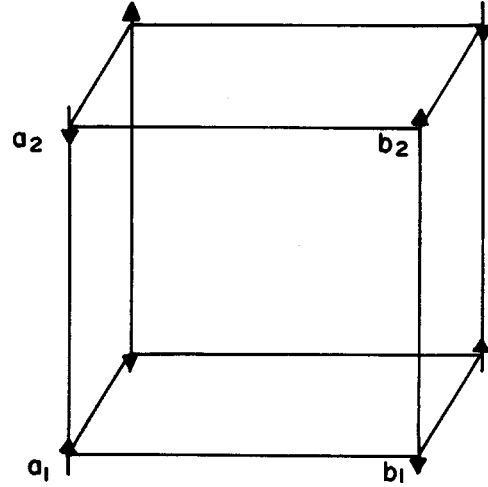


FIG. 1. Four sublattices of a bilayer system with spins up and down at label  $a_1$  (layer 1),  $b_2$  (layer 2) and  $a_2$  (layer 2),  $b_1$  (layer 1), respectively. Here the suffix shows the layer indices.

note the creation (annihilation) operator corresponding to the spinless fermion and  $s_{i\sigma l}^+$  ( $s_{i\sigma l}$ ) denote the spin operator at the site  $i$  of the  $l$ th layer. Then the electron operator may be written as

$$c_{i\sigma l} = f_{il} s_{i\sigma l}^+ \quad \text{and} \quad c_{i\sigma l}^+ = f_{il}^+ s_{i\sigma l} \quad (6)$$

and the constraint on each site is given by

$$f_{il}^+ f_{il} + s_{i\sigma l}^+ s_{i\sigma l} = 1. \quad (7)$$

To describe a bilayer cuprate system, we consider the four-sublattice model. These four sublattices are labeled by  $a_l, b_l$  where  $l=1,2$  (Fig. 1). In fact, the ground state of the bilayer cuprate is antiferromagnetic, which may be composed of four sublattices having spin up, say, at  $a_1$  (layer 1) and  $b_2$  (layer 2) sublattices and spin down  $b_1$  (layer 1) and  $a_2$  (layer 2) sublattices as shown in Fig. 1. Using Eq. (6) the Hamiltonian (1) can be written in the form

$$H = - \sum_{l, \sigma, i \neq j, l'} t_{ll'} L_{ll'} f_{il}^+ f_{jl'} s_{i\sigma l} s_{j\sigma l'} + \sum_{l, l', \sigma, \sigma', i \neq j, l'} [J_{ll'}, L_{ll'} \sigma \sigma' f_{il}^+ f_{jl'} f_{j\sigma' l'}^+ f_{i\sigma l}^-] \times \{ s_{i\sigma l} s_{i\sigma' l}^+ s_{j\sigma' l'} s_{j\sigma l}^+ + \frac{1}{2} s_{i\sigma l} s_{i-\sigma l}^+ s_{j\sigma' l'} s_{j\sigma' l'}^+ \} + \sum_{l, i} \lambda_{l, i} \left[ \sum_{\sigma} f_{il}^+ f_{il} s_{i\sigma l}^+ s_{i\sigma l} - 1 \right]. \quad (8)$$

Here  $\lambda_{l, i}$  is the Lagrange multiplier, which takes care of the constraints imposed by Eq. (7). We may generalize the Schwinger boson spin representation to large  $S$ ; the constraint (7) is replaced by

$$s_{i\uparrow}^{\dagger} s_{i\uparrow} + s_{i\downarrow}^{\dagger} s_{i\downarrow} = 2S. \quad (9)$$

There are now  $2S$  spin- $\frac{1}{2}$  Schwinger bosons on each site. In the large  $S$  limit we may consider mean field theory approximation that is equivalent to the saddle-point expansion of the functional integral.<sup>37</sup> A stable mean field solution occurs when the saddle points are given by

$$X=0, \quad Y=\pm\sqrt{2S}, \quad \lambda=0, \quad (10a)$$

$$X=\pm\sqrt{2S}, \quad Y=0, \quad \lambda=0, \quad (10b)$$

or by

$$X=\pm\sqrt{S}, \quad Y=\pm\sqrt{S}, \quad \lambda=0. \quad (10c)$$

Here  $X=s_{i_1\uparrow a_1}^{(+)}=s_{j_1\downarrow b_1}^{(+)}=s_{i_2\downarrow a_2}^{(+)}=s_{j_2\uparrow b_2}^{(+)}$  and

$$Y=s_{i_1\downarrow a_1}^{(+)}=s_{j_1\uparrow b_1}^{(+)}=s_{i_2\uparrow a_2}^{(+)}=s_{j_2\downarrow b_2}^{(+)}. \quad (10c)$$

The first two states [Eqs. 10(a) and 10(b)] correspond to an antiferromagnetic state ( $X \neq Y$ ) while the third state corresponds to the ferromagnetic state ( $X = Y$ ). In the present calculation we have taken the antiferromagnetic ground state of the system because it is well known that the insulating undoped state of cuprate system is antiferromagnetic. The effective Hamiltonian corresponding to the antiferromagnetic ground state [Eqs. 10(a) and 10(b)] may be written in the form

$$\begin{aligned} H = & - \sum_{l, i_1 \neq j_{l'}} t_{ll'} L_{ll'} f_{il}^{\dagger} f_{j_{l'}} (s_{i_1\uparrow a_1}^{\dagger} + s_{j_{l'}\downarrow b_{l'}}^{\dagger}) \\ & + \sum_{\substack{l, l', \\ i_1 \neq j_{l'}}} [J_{ll'} L_{ll'} \sigma \sigma' f_{il}^{\dagger} f_{j_{l'}} f_{i_1\uparrow a_1}^{\dagger} \{ (s_{i_1\uparrow a_1}^{\dagger} s_{i_1\uparrow a_1}^{\dagger} \\ & + s_{j_{l'}\downarrow b_{l'}}^{\dagger} s_{j_{l'}\downarrow b_{l'}}^{\dagger}) + (s_{i_1\uparrow a_1}^{\dagger} s_{j_{l'}\downarrow b_{l'}}^{\dagger} + s_{i_1\uparrow a_1}^{\dagger} s_{j_{l'}\downarrow b_{l'}}^{\dagger}) \}]. \end{aligned} \quad (11)$$

We express the above Hamiltonian in the momentum representation using the following Fourier transformations:

$$\begin{pmatrix} t_{\parallel}(\mathbf{R}_i - \mathbf{R}_j) \\ t_{\perp} \end{pmatrix} = \sum_{\mathbf{k}} \begin{pmatrix} \varepsilon_{\mathbf{k}} \\ \varepsilon_{\perp \mathbf{k}} \end{pmatrix} \exp(-i\mathbf{k} \cdot (\mathbf{R}_i - \mathbf{R}_j)), \quad (12)$$

$$\begin{pmatrix} J_{\parallel}(\mathbf{R}_i - \mathbf{R}_j) \\ J_{\perp} \end{pmatrix} = \sum_{\mathbf{q}} \begin{pmatrix} J_{\parallel}(\mathbf{q}) \\ J_{\perp}(\mathbf{q}) \end{pmatrix} \exp(-i\mathbf{q} \cdot (\mathbf{R}_i - \mathbf{R}_j)), \quad (13)$$

$$f_i = \sum_{\mathbf{k}} f_{\mathbf{k}} \exp\{i\mathbf{k} \cdot \mathbf{R}_i\}, \quad (14)$$

$$s_i = \sum_{\mathbf{q}} s_{\mathbf{q}} \exp\{i\mathbf{q} \cdot \mathbf{R}_i\}. \quad (15)$$

In Eqs. (12) and (13)  $\varepsilon_{\mathbf{k}}$  and  $J_{\parallel}(\mathbf{q})$  are, respectively, given by

$$\varepsilon_{\mathbf{k}} = -2t_{\parallel} \{ \cos k_x + \cos k_y \} \quad (16)$$

and

$$J_{\parallel}(\mathbf{q}) = -2z_{ab} J_{\parallel} \{ \cos q_x + \cos q_y \}. \quad (17)$$

Here  $z_{ab}$  ( $=4$ ) is the number of the nearest neighbors of Cu within the  $\text{CuO}_2$  plane.  $\varepsilon_{\mathbf{k}}$  is the energy dispersion for the Cu- $\text{O}_2$  plane. With the help of Eqs. (12)–(15), Eq. (11) can be written as

$$\begin{aligned} H = & - \sum_{l, k, k', q} L_{ll'} \{ f_{lk+q}^{\dagger} f_{lk} (\varepsilon_{ll'k} s_{qa_1}^{-} + \varepsilon_{ll'k+q} s_{-qb_1}^{+}) \\ & + f_{lk-q}^{\dagger} f_{lk} (\varepsilon_{ll'k-q} s_{qa_1}^{+} + \varepsilon_{ll'k} s_{-qb_1}^{-}) \} \\ & + \sum_{\substack{l, l', \\ k, k', q}} [J_{ll'} L_{ll'} f_{lk+q}^{\dagger} f_{lk} f_{l'k'-q}^{\dagger} f_{l'k'} \{ (s_{qa_1}^{+} s_{qa_1}^{-} \\ & + s_{-qb_{l'}}^{+} s_{-qb_{l'}}^{-}) + (s_{qa_1}^{+} s_{-qb_{l'}}^{+} + s_{qa_1}^{-} s_{-qb_{l'}}^{-}) \}]. \end{aligned} \quad (18)$$

The spectral function, density of states, and hole density can be derived from the Green's function. We use the following Green's functions corresponding to the spinless fermions:

$$G_{lkk'}(\omega) = \langle \langle f_{lk} | f_{l'k'}^{\dagger} \rangle \rangle \quad (l=1,2) \quad (19a)$$

and

$$G_{\perp kk'}(\omega) = \langle \langle f_{2k} | f_{1k'}^{\dagger} \rangle \rangle. \quad (19b)$$

Here,  $\omega$  denotes the energy.  $G_{lkk'}(\omega)$  corresponds to the motion of spinless fermions in the same layer while  $G_{\perp kk'}(\omega)$  corresponds to the motion from one layer to the other layer of the unit cell. In solving the equation of motion, we obtain 16 equations for different Green's functions. We have solved all the equations simultaneously and obtain final equation of motion for Green's functions  $G_{lkk'}(\omega)$  and  $G_{\perp kk'}(\omega)$ , which read

$$\begin{aligned} [\omega - \Sigma_l(k, \omega)] G_l(k, \omega) = & \delta_{ll'} + \Sigma_{l'}(k, \omega) G_{l'}(k, \omega) \\ & + \phi_{l'} \quad (l, l' = 1, 2) \end{aligned} \quad (20)$$

where  $\Sigma_l(k, \omega)$  is the self-energy. The expression of the self-energy  $\Sigma_l(k, \omega)$  and  $\phi_{l'}$  is given in the Appendix.

The electronic spectral function  $A(k, \omega)$  of the system is defined as the imaginary part of the Green's function

$$A(k, \omega) = -2 \text{Im} G(k, \omega). \quad (21)$$

The density of states (DOS) of the system is obtained by integrating the spectral function for all the possible  $\mathbf{k}$  values,

$$N(\omega) = \int_{-\pi}^{\pi} \int_{-\pi}^{\pi} A(k, \omega) dk_x dk_y. \quad (22)$$

Here, we have integrated the spectral function over  $k_x$  and  $k_y$  values because we have not considered the interbilayer interactions.<sup>34</sup> Finally, the hole density ( $\delta$ ) is obtained by integrating the density of states over the occupied energy states,

$$\delta = \int_{-\infty}^{\mu} N(\omega) d\omega. \quad (24)$$

### III. RESULTS AND DISCUSSION

We have calculated the spectral function, the imaginary part of self-energy, the density of states, and the hole density of bilayer cuprates. In the present calculations we have taken the in-plane hopping integral  $t_{\parallel} = 0.4$  eV and the in-plane exchange coupling  $J_{\parallel} = 0.3 t_{\parallel}$ . The cuprates have values of these parameters in this range.<sup>35</sup> The values of the hopping integral  $t_{\perp}$  for the coupling of two layers within the same cell, the intrabilayer exchange coupling  $J_{\perp}$  expressed in terms of  $t_{\parallel}$  and  $J_{\parallel}$ , and the anisotropy parameter  $r$  are given by using the standard relations<sup>35</sup>

$$r = J_{\parallel} / J_{\perp} = t_{\parallel}^2 / t_{\perp}^2. \quad (24)$$

It may be noted that the anisotropy parameter  $r$  approaching infinity represents two isolated (uncoupled)  $\text{CuO}_2$  layers since for  $r \rightarrow \infty$ ,  $J_{\perp}$  and  $t_{\perp} \rightarrow 0$ . This case effectively corresponds to a behavior of the single layer cuprates. On the other hand,  $r = 1$  represents an isotropic three-dimensional (3D) system where the intrabilayer interactions are as strong as the in-plane interactions. The  $\mathbf{k}$  dependence of  $\varepsilon_{\perp \mathbf{k}}$  and the  $\mathbf{q}$  dependence of  $J_{\perp}(\mathbf{q})$  are taken such that these agree with the experimental measurements of angle-resolved photoemission which shows that there is no hopping of holes between the two layers along the  $k_x = k_y$  direction.<sup>32</sup> This means that  $\varepsilon_{\perp \mathbf{k}} = 0$  for  $k_x = k_y$ . A reasonable form of  $\varepsilon_{\perp \mathbf{k}}$  which satisfies this requirement has been suggested by Chakravarty *et al.*,<sup>32</sup>

$$\varepsilon_{\perp \mathbf{k}} = -2t_{\perp} \{ \cos k_x - \cos k_y \}^2, \quad (25)$$

$$J_{\perp}(\mathbf{q}) = -2z_c J_{\perp} \cos q_z, \quad (26)$$

where  $z_c$  is the number of nearest-neighbor Cu spins between two layers along the  $z$  direction.

We have calculated the spectral function and the density of states for different values of the anisotropy parameters  $r = \infty$ ,  $r = 10$ , and  $r = 6.7$ . We found that for  $r = 6.7$  the spectral properties show only about 5% variation from the case of  $r = 10.0$ . So we have not presented and discussed the calculations for anisotropy ratio  $r = 6.7$ .

We present results of our calculations for spectral function  $A(\mathbf{k}, \omega)$  at  $(k_x, k_y)$  points  $(0, 0)$ ,  $(\pi/2, \pi/2)$ ,  $(\pi, \pi)$ ,  $(\pi, \pi/2)$ ,  $(\pi, 0)$ , and  $(\pi/2, 0)$  for  $r = \infty$  in Fig. 2 and for  $r = 10$  in Figs. 3 and 4. For the doping parameter  $\delta = 0.1$  and temperature  $T = 0.05 t_{\parallel}$ , we observe from Fig. 2 that  $A(\mathbf{k}, \omega)$  consists of coherent quasiparticle peaks with a broad incoherent background for all the values of  $\mathbf{k}$  chosen by us. It is also observed from Fig. 2 that for a single layer going from the  $(0, 0)$  direction to the  $(\pi, 0)$  direction or from  $(0, 0)$  to  $(\pi, \pi)$  there is an appearance of the electronlike quasiparticle character above the Fermi energy. We do not notice any coherent peak in the spectral function at the  $(\pi, 0)$  point. Ino *et al.*<sup>10</sup> and Sato *et al.*<sup>6</sup> have also observed that spectral function shows a featureless  $\omega$  variation of  $A(\mathbf{k}, \omega)$  near  $(\pi, 0)$  for an

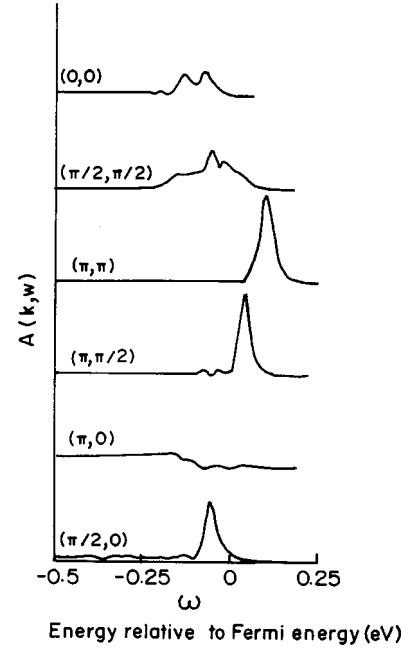


FIG. 2. Spectral function  $A(\mathbf{k}, \omega)$  for a single layer ( $r \rightarrow \infty$ ) system for different  $\mathbf{k}$  points with  $T = 0.05 t_{\parallel}$  and  $\delta = 0.1$ .

underdoped single layer system. Features of  $A(\mathbf{k}, \omega)$  for the bilayer cuprates are presented in Fig. 3 for  $T = 0.05 t_{\parallel}$  and  $\delta = 0.1$ . These results are obtained by taking the form of intrabilayer hopping given by Eq. (25). Comparing the spectral weight for a single layer and bilayer cuprates at different  $\mathbf{k}$  values, it is evident from Figs. 2 and 3 that maximum change in the electronic part of the spectral weight occurs for the  $(\pi, 0)$  point of the Brillouin zone. The spectral weight shows sharp features above the Fermi energy at the  $(\pi, 0)$  point, which was absent for uncoupled layers. The reason for this

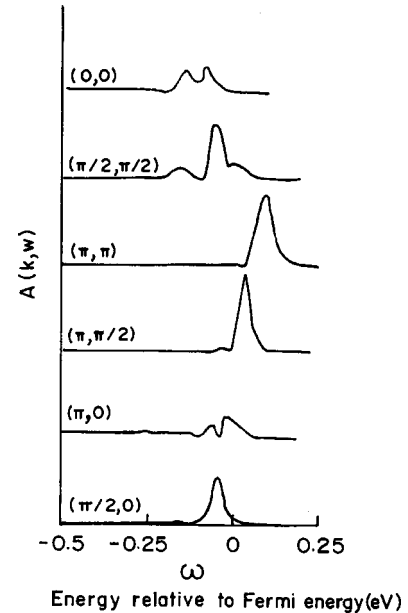


FIG. 3. Spectral function  $A(\mathbf{k}, \omega)$  for a bilayer system ( $r = 10.0$ ) for different  $\mathbf{k}$  points with  $T = 0.05 t_{\parallel}$  and  $\delta = 0.1$ .

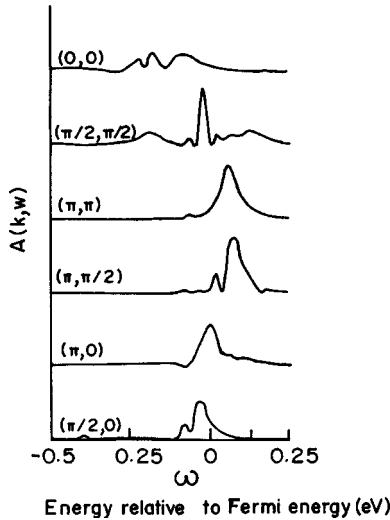


FIG. 4. Spectral function  $A(\mathbf{k}, \omega)$  for a bilayer system ( $r = 10.0$ ) for different  $\mathbf{k}$  points with  $T = 0.1t_{\parallel}$  and  $\delta = 0.2$ .

change should be due to the bilayer coupling. Because of the form chosen for  $\varepsilon_{\perp}$  in Eq. (25), the maximum change in the spectral function will occur at  $(\pi, 0)$  point. We observe that changes in the spectral function for a coupled bilayer system compared to uncoupled layers are small at points  $(\pi, \pi/2)$  and  $(\pi/2, 0)$ . From Fig. 3 it is also clear that for the underdoped bilayer system the peak at the points  $(\pi/2, \pi/2)$ ,  $(\pi, \pi)$ , and  $(\pi, \pi/2)$  is sharp while the peak at  $(\pi, 0)$  is broad and suppressed. Kim and co-workers<sup>40</sup> have observed a similar feature by using ARPES measurements. We also observe a sharper peak curve for the spectral function at the  $(\pi/2, \pi/2)$  point near the Fermi energy for underdoped coupled bilayers, but for  $r = \infty$  (uncoupled layers) this peak is relatively suppressed (Fig. 2). The ARPES studies carried out by Ino *et al.*<sup>10</sup> have also shown this behavior. They suggest that the difference between the spectral function of uncoupled layers and coupled layers at  $(\pi/2, \pi/2)$  is related to the formation of dynamical strips in the single layer system.

We now turn to the presentation of our results of the spectral function for a higher temperature and relatively larger doping concentration ( $T = 0.1t_{\parallel}$  and  $\delta = 0.2$ ). The results are plotted in Fig. 4. By comparing Figs. 3 and 4, we see that on increasing the doping from  $\delta = 0.10$  (underdoped) to  $\delta = 0.2$  (slightly over doped) the quasiparticle peak at  $(\pi, 0)$  moves closer to the Fermi energy and becomes sharper and more intense. These results are in accord with the observations of Shen and Schriffer<sup>19</sup> for bilayer cuprates. Comparing Figs. 3 and 4, we find that the spectral function shows a little broadening as  $\delta$  increases. This is in qualitative agreement with the predictions of Baskaran, Zou, and Anderson<sup>41</sup> and Wang and Kotliar<sup>42</sup> where they have suggested that the broadening in the spectral function is directly related to the doping concentration.

From Figs. 2, 3, and 4, one can see that the bilayer coupling significantly affects the electronic states of bilayer cuprates. However, we do not find the splitting of electronic states along the  $(\pi, 0)$  direction up to the hole concentration  $\delta = 0.2$ . In view of the recent ARPES experiment,<sup>16</sup> we study the behavior of the spectral function specifically along the

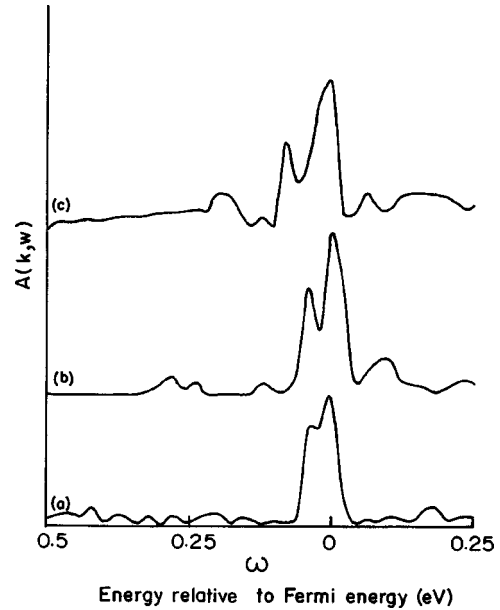


FIG. 5. Spectral function  $A(\mathbf{k}, \omega)$  for a bilayer system ( $r = 10.0$ ) along the  $(\pi, 0)$  direction with  $T = 0.15t_{\parallel}$  for different values of hole concentration. (a)  $\delta = 0.24$ , (b)  $\delta = 0.28$ , and (c)  $\delta = 0.32$ .

$(\pi, 0)$  direction for a higher doping concentration (heavily overdoped). We observed that for the hole concentration  $\delta = 0.24$ , the quasiparticle peak of the spectral function along the  $(\pi, 0)$  direction shows a sign of the splitting of electronic states [Fig. 5(a)]. On increasing the hole concentration to  $\delta = 0.28$ , the quasiparticle electronic states clearly splits into two peaks [Fig. 5(b)]. These results are qualitatively in accord with the recent ARPES observation by Feng *et al.*,<sup>16</sup> where they have observed that the electronic states of heavily overdoped bilayer cuprates (Bi2212) splits into bonding and antibonding states along the  $(\pi, 0)$  direction. On further increasing the doping concentration to  $\delta = 0.32$  (heavily overdoped regime), we observe that the splitting of the electronic states is more pronounced than that for  $\delta = 0.28$  [Fig. 5(c)]. Here we also observed that the spacing between two peaks of electronic states is increased by a factor of 2 while increasing the doping concentration from  $\delta = 0.28$  to  $\delta = 0.32$ . However, the quantitative strength of the bilayer splitting observed here (16 meV,  $\delta = 0.32$ ) is lesser than the experimentally observed value (80 meV) for heavily overdoped bilayer cuprates. The other theoretical calculation carried out by using the bilayer Hubbard model also suffers with a similar discrepancy,<sup>33</sup> i.e., a lower value of bilayer splitting (40 meV). Their calculation suggests that for a heavily overdoped system (strong bilayer hopping) one should consider a weak correlation (low  $U$ ) rather than a strong correlation (higher  $U$ ). Moreover, the discrepancy in our calculation may be due to the inadequacy of the slave-fermion approach considered here, as it deals with strong correlations ( $U \rightarrow \infty$ ) even for the higher doping regime. We see that this splitting of states occurs only at a higher doping concentration. The reason for this peak splitting for a higher doping concentration is that on increasing the doping concentration, the coupling between the two  $\text{CuO}_2$  layers is effectively enhanced.

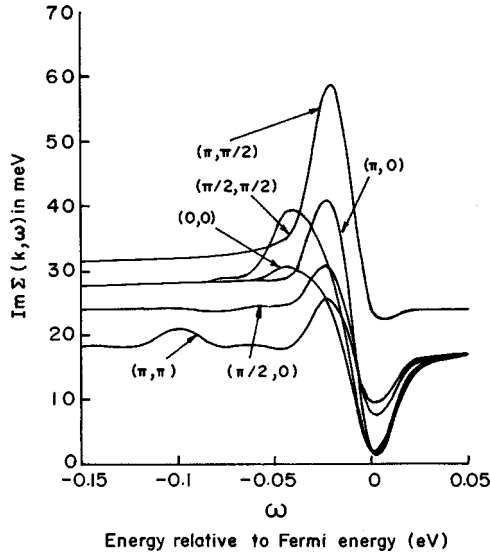


FIG. 6. Imaginary part of the self-energy for different  $k$  points corresponding to  $T=0.05t_{\parallel}$ ,  $r=10.0$ , and  $\delta=0.1$ .

From the knowledge of the spectral function at various  $k$  points in the Brillouin zone, one can construct the Fermi surface and analyze the effect of bilayer coupling on it. This will also give an idea about the nature of the Fermi surface. Our objective in this paper is limited to studying the effects of intralayer couplings on the spectral function of coupled and uncoupled bilayer cuprates.

Next, we plot the imaginary part of the self-energy  $\Sigma_1''(\mathbf{k}, \omega)$  for  $\delta=0.1$ ,  $r=10.0$ , and  $T=0.05 t_{\parallel}$  and  $(k_x, k_y) = (0, 0), (\pi/2, 0), (\pi, 0), (\pi, \pi/2), (\pi/2, \pi/2),$  and  $(\pi, \pi)$  points of the Brillouin zone are given in Fig. 6. The imaginary part of the self-energy as a function of energy  $\omega$  shows a complicated behavior. In Fig. 6 we see that  $\Sigma_1''(\mathbf{k}, \omega)$  shows a strong  $k$  dependence. Many other theoretical calculations also show strong  $k$  dependence of  $\Sigma_1''(\mathbf{k}, \omega)$ <sup>2,19,42-44</sup> although theories like the marginal Fermi-liquid theory<sup>43</sup> ignore the  $\mathbf{k}$  dependence of  $\Sigma_1''$ . We note that the behavior of  $\Sigma_1''(\mathbf{k}, \omega)$  is very different for  $\omega < 0$  compared to  $\omega > 0$  for all  $k$ . For  $\omega < 0$  (near  $\omega \sim 0$ )  $\Sigma_1''$  shows an  $\omega^\alpha$ -like dependence with  $1.2 < \alpha < 1.5$ . Several experiments have shown such a power-law behavior for  $\Sigma_1''(\mathbf{k}, \omega)$  at low  $\omega$ .<sup>46-48</sup> Theoretical analyses also support a power-law behavior of  $\Sigma_1''(\mathbf{k}, \omega)$ . For example Stojkovic *et al.*<sup>44</sup> argue that spin fluctuations are responsible for the dependence of  $\Sigma_1''(\mathbf{k}, \omega)$  on  $\omega$ . Anderson<sup>1</sup> suggests that this power law dependence is arising from the fact that in cuprates the electrons behave like a two-dimensional Luttinger liquid. Lal<sup>45,46</sup> obtained a power-law behavior of  $\Sigma_1''(\mathbf{k}, \omega)$  using a model that includes Coulomb interaction and electron-phonon interaction. Very recently Pratap and collaborators<sup>35</sup> have also obtained a  $\omega^\alpha$ -like variation of  $\Sigma_1''(\mathbf{k}, \omega)$  by using a perturbative approach within the  $t$ - $t'$ - $J$  model. Several experiments have shown such power-law behavior for  $\Sigma_1''(\mathbf{k}, \omega)$  at low  $\omega$ .<sup>46-50</sup>

In Fig. 7 we show how the single-particle density of states (DOS),  $N(\omega)$  changes on doping. For the underdoped system  $\delta=0.075$ , we observed a peak around  $\omega < 0$  and a background due to incoherent hole motion dominates for  $\omega \ll 0$

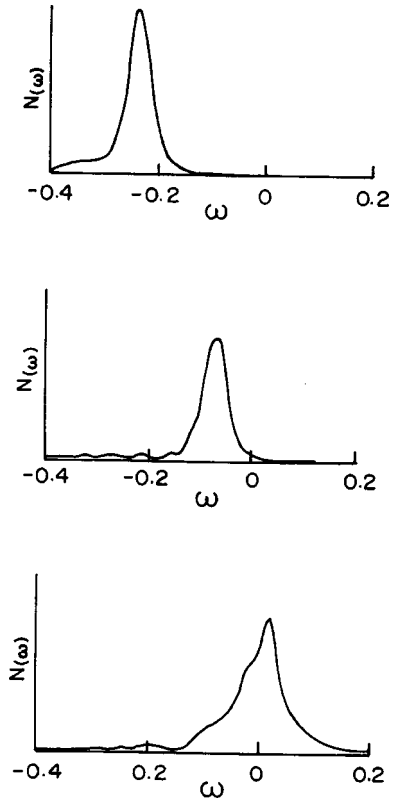


FIG. 7. Density of states  $N(\omega)$  for a bilayer system ( $r=10.0$ ) for (a)  $T=0.05t_{\parallel}$  and  $\delta=0.075$ , (b)  $T=0.05t_{\parallel}$  and  $\delta=0.1$ , and (c)  $T=0.1t_{\parallel}$  and  $\delta=0.2$ .

[Fig. 7(a)]. At such low doping  $N(\omega)$  is negligible for  $\omega > 0$ . On increasing hole concentration to  $\delta=0.10$  the incoherent background due to holes reduces in intensity while the coherent part near the Fermi energy gets widened [Fig. 7(b)]. On further increasing the doping concentration to  $\delta=0.2$  and the temperature to  $T=0.1 t_{\parallel}$ , we see that  $N(\omega)$  remain appreciable for  $\omega > 0$  [Fig. 7(c)].

Finally, we present the results for the hole density ( $\delta$ ) as a function of temperature for different values of the chemical potential ( $\mu$ ) in Fig. 8. We present the results of hole density corresponding to the anisotropic parameter  $r=10.0$  and the chemical potential  $\mu = -1.55, -2.0,$  and  $-2.1$ . From this

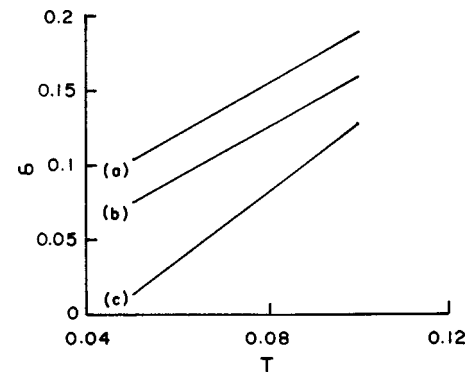


FIG. 8. Variation of the hole density ( $\delta$ ) with temperature ( $T$ ) for  $r=10.0$  and (a)  $\mu = -1.55$ , (b)  $\mu = -2.0$ , and (c)  $\mu = -2.1$ . Here  $T$  is given in the term of  $t_{\parallel}$ .

figure, one can infer that on increasing the temperature, the number of holes increases. It is clear that for the lower values of  $\mu$ , the rate of the increase of the hole concentration with temperature is higher. From the figure it can also be seen that these hole concentration curves for different values of  $\mu$  come close to each other at higher values of  $T$ . Jaklic and collaborators<sup>29–32</sup> also arrived with a qualitatively similar result in their calculations.

#### IV. CONCLUSIONS

In this paper we have calculated the spectral function of a bilayer cuprate with and without coupling between two Cu-O<sub>2</sub> layers in the same unit cell for various values of momentum, hole concentration, temperature, and the anisotropy factor. It is found that in moving from the origin of  $k$  space (0,0) to the  $(\pi, 0)$  direction or (0,0) to the  $(\pi, \pi)$  direction the spectral function shows that the electronic quasiparticle character increases above the Fermi energy. The coupling between the two neighboring planes in the same unit cell is seen to influence the form and the shape of the spectral function. In particular, we found that the maximum effect of coupling between the layers on the spectral function is around the (0,0) to  $(\pi, 0)$  direction. The spectral function around the  $(\pi, 0)$  direction becomes sharp and moves towards the Fermi energy.

The maximum effect of bilayer coupling on the spectral function is found to be at the  $(\pi, 0)$  point. The spectral function around  $(\pi, 0)$  becomes sharp and moves towards the Fermi energy. In our calculation, we do not find the splitting of a quasiparticle peak up to the hole concentration  $\delta=0.2$ . Our calculation shows a splitting of electronic states at a higher doping concentration ( $\delta \geq 0.24$ ) as observed in recent ARPES experiments. However, the quantitative strength of the splitting seen in our calculation is less than that observed in the ARPES experiments.<sup>16</sup> In the present paper we have also studied the contribution of the imaginary part of self-energy, which is found to be strongly  $k$  dependent, and we show a  $\omega^\alpha$  dependence on energy.

#### ACKNOWLEDGMENT

The Department of Science and Technology, Government of India, via Grant No. SP/S2/M-07/2001, supported this work financially.

#### APPENDIX

In Eq. (20), the expression for self-energy  $\Sigma_l$  is given by

$$\Sigma_l(k, \omega) = \sum_q \frac{\xi_l(k, \omega)}{\omega}, \quad (\text{A1})$$

where

$$\xi_l(k, \omega) = \sum_{l', q} \{ \varepsilon_{k-q} E_{a-}^{ll'} + \varepsilon_{k+q} E_{b-}^{ll'} + \varepsilon_k (E_{a+}^{ll'} + E_{b+}^{ll'}) \}. \quad (\text{A2})$$

In the above equation the various energy parameters  $E$  are given by

$$E_{a-}^{11} = \varepsilon_{k+q} \langle s_{a_1 a_1}^{+-} \rangle, \quad (\text{A3a})$$

$$E_{b+}^{11} = \varepsilon_{k-q} \langle s_{b_1 a_1}^{++} \rangle, \quad (\text{A3b})$$

$$E_{a+}^{11} = \varepsilon_{k+q} \langle s_{a_1 b_1}^{++} \rangle, \quad (\text{A3c})$$

$$E_{b-}^{11} = \varepsilon_{k+q} \langle s_{b_1 b_1}^{-+} \rangle, \quad (\text{A3d})$$

$$E_{a-}^{12} = \varepsilon_{\perp k+q} \langle s_{a_1 b_2}^{--} \rangle + \varepsilon_{\perp k} \langle s_{a_1 a_1}^{-+} \rangle, \quad (\text{A3e})$$

$$E_{b+}^{12} = \varepsilon_{\perp k} \langle s_{b_2 a_1}^{++} \rangle + \varepsilon_{\perp k+q} \langle s_{b_2 b_2}^{+-} \rangle, \quad (\text{A3f})$$

$$E_{b-}^{12} = \varepsilon_{\perp k-q} \langle s_{b_1 b_1}^{-+} \rangle + \varepsilon_{\perp k+q} \langle s_{b_1 a_2}^{+-} \rangle, \quad (\text{A3g})$$

$$E_{a+}^{12} = \varepsilon_{\perp k-q} \langle s_{a_2 a_2}^{+-} \rangle, \quad (\text{A3h})$$

$$E_{a-}^{21} = \varepsilon_{\perp k} \langle s_{a_1 b_1}^{--} \rangle, \quad (\text{A3i})$$

$$E_{b+}^{21} = \varepsilon_{\perp k-q} \langle s_{b_1 a_2}^{++} \rangle, \quad (\text{A3j})$$

$$E_{a+}^{21} = \varepsilon_{\perp k-q} \langle s_{a_1 b_2}^{++} \rangle, \quad (\text{A3k})$$

$$E_{b-}^{21} = \varepsilon_{\perp k} \langle s_{b_1 a_1}^{--} \rangle + \varepsilon_{\perp k-q} \langle s_{b_1 a_2}^{-+} \rangle, \quad (\text{A3l})$$

$$E_{a-}^{22} = \varepsilon_k \langle s_{a_1 b_2}^{--} \rangle, \quad (\text{A3m})$$

$$E_{b+}^{22} = \varepsilon_k \langle s_{b_2 b_2}^{+-} \rangle + \varepsilon_{k-q} \langle s_{b_2 a_2}^{++} \rangle, \quad (\text{A3n})$$

$$E_{b-}^{22} = \varepsilon_{k+q} \langle s_{b_1 b_1}^{-+} \rangle + \varepsilon_k \langle s_{b_1 a_2}^{+-} \rangle, \quad (\text{A3o})$$

$$\text{and } E_{a+}^{22} = \varepsilon_k \langle s_{a_2 a_2}^{++} \rangle. \quad (\text{A3p})$$

In Eq. (A3) the  $\langle s_{ll} \rangle$  are the correlation functions corresponding to the spin operators. To obtain an expression for these spin correlation functions we have calculated the relevant spin Green's function. From these spin Green functions we obtained expressions for spin correlation functions which are given by

$$\langle\langle s_{a_1 a_1}^{+-} \rangle\rangle = S' [B(-n, -m) + B(-n, m)], \quad (\text{A4a})$$

$$\langle\langle s_{b_1 a_1}^{--} \rangle\rangle = S' [B(-n, -m) - B(-n, m)], \quad (\text{A4b})$$

$$\langle\langle s_{b_2 a_1}^{--} \rangle\rangle = S' [L(-n, -m) + L(-n, m)], \quad (\text{A4c})$$

$$\langle\langle s_{a_2 a_1}^{--} \rangle\rangle = S' [L(-n, -m) - L(-n, m)], \quad (\text{A4d})$$

$$\langle\langle s_{b_1 b_1}^{+-} \rangle\rangle = S' [B(n, m) + B(n, -m)], \quad (\text{A4e})$$

$$\langle\langle s_{a_1 b_1}^{--} \rangle\rangle = S' [B(n, m) - B(n, -m)], \quad (\text{A4f})$$

$$\langle\langle s_{a_2 b_1}^{--} \rangle\rangle = S' [L(n, m) + L(n, -m)], \quad (\text{A4g})$$

$$\langle\langle s_{b_2 b_1}^{+-} \rangle\rangle = S' [L(n, m) - L(n, -m)], \quad (\text{A4h})$$

where  $S' = S/2\pi$ ,

$$B(n, m) = (\omega + n + m) / [(\omega + n + m)^2 - p^2], \quad (\text{A5})$$

$$L(n, m) = p / [(\omega + n + m)^2 - p^2], \quad (\text{A6})$$

$$n = 8S^2 \sum_k \{J_{\parallel}(q)F_{11} + J_{\perp}(q)F_{12}\}, \quad (\text{A7})$$

$$m = 2S^2 \sum_k \{J_{\parallel}(q)F_{11}\}, \quad (\text{A8})$$

$$p = 2S^2 \sum_k \{J_{\perp}(q)F_{21}\}. \quad (\text{A9})$$

We can obtain the expressions for various spin correlation functions by integrating and taking an imaginary part of the corresponding Green's function [given in Eq. (A4)]. For example,

$$\langle s_{pp}^{xx} \rangle = -\text{Im} \int \langle\langle s_{pp}^{xx} \rangle\rangle d\omega. \quad (\text{A10})$$

In Eq. (20)  $\phi_1$  and  $\phi_2$  are given by

$$\phi_1 = \sum_{k,q} (\eta_1 F_{11} + \eta_2 F_{12}), \quad (\text{A11a})$$

$$\phi_2 = \sum_{k,q} (\eta_1 F_{22} + \eta_2 F_{21}), \quad (\text{A11b})$$

where

$$\eta_l = -5S^2 J_l'(\kappa) + 4S J_l'(q) \sum_{l'} (s_{a_l a_{l'}}^{+-} + s_{b_l b_{l'}}^{+-})$$

$$+ 5J_l'(q) \sum_{l', l''} (s_{a_l a_{l''}}^{++} + s_{a_l b_{l''}}^{--}) D_{ll' l''}, \quad (\text{A12})$$

$$D_{ll' l''} = \delta_{l1} \delta_{l' l''} + \delta_{l2} (1 - \delta_{l' l''}), \quad (\text{A13})$$

$$J_l' = J_{l' l''} D_{ll' l''}. \quad (\text{A14})$$

Equations (A7)–(A9) and (A11) involve the Green's functions  $F_{11}$ ,  $F_{12}$ , and  $F_{21}$ . These Green's functions are the products of four fermion operators. We obtain the following expressions for these Green's functions using a suitable decoupling approximation<sup>39</sup>:

$$F_{11} = \langle\langle f_{1k-q} f_{1k-q}^+ | f_{1k} f_{1k}^+ \rangle\rangle = \left[ \frac{n(\varepsilon_{k-q}) - n(\varepsilon_k)}{\omega + \varepsilon_{k-q} - \varepsilon_k + i0} \right], \quad (\text{A15})$$

$$F_{22} = \langle\langle f_{2k-q} f_{2k-q}^+ | f_{2k} f_{1k}^+ \rangle\rangle = \sum_2 \left[ \frac{n(\Sigma_1)}{(\Sigma_1 - \varepsilon_k)(\Sigma_1 - \omega - \varepsilon_{k-q})} + \frac{n(\varepsilon_k)}{(\varepsilon_k - \Sigma_1)(\varepsilon_k - \omega - \varepsilon_{k-q})} + \frac{n(\varepsilon_{k-q})}{(\omega + \varepsilon_{k-q} - \Sigma_1)(\omega + \varepsilon_{k-q} - \varepsilon_k)} \right], \quad (\text{A16})$$

$$F_{12} = F_{21} = \langle\langle f_{2k+q} f_{2k}^+ | f_{1k} f_{1k+q} \rangle\rangle = \sum_2 \left[ \frac{n(\Sigma_1)}{\omega(\Sigma_1 - \varepsilon_k)(\Sigma_1 + \omega - \varepsilon_{k-q})} + \frac{n(\varepsilon_k)}{(\varepsilon_k - \Sigma_1)(\varepsilon_k + \omega - \varepsilon_{k-q})(\varepsilon_k + \omega - \Sigma_1)} + \frac{n(\Sigma_1)}{\omega(\omega + \varepsilon_k - \Sigma_1)(\Sigma_1 - \varepsilon_{k-q})} + \frac{n(\varepsilon_{k+q})}{(\varepsilon_{k+q} - \Sigma_1)(\varepsilon_{k+q} + \omega - \varepsilon_{k-q})(\omega + \Sigma_1 - \varepsilon_{k+q})} \right]. \quad (\text{A17})$$

In the course of discussion we found that the spin correlation operators have the following symmetry:

$$\langle s_{a_1 a_1}^{+-} \rangle = \langle s_{a_2 a_2}^{+-} \rangle = \langle s_{b_1 b_1}^{-+} \rangle = \langle s_{b_2 b_2}^{-+} \rangle, \quad (\text{A18a})$$

$$\langle s_{b_1 a_1}^{--} \rangle = \langle s_{b_2 a_2}^{--} \rangle = \langle s_{a_1 b_1}^{++} \rangle = \langle s_{a_2 b_2}^{++} \rangle, \quad (\text{A18b})$$

$$\langle s_{b_2 a_1}^{--} \rangle = \langle s_{b_1 a_2}^{--} \rangle = \langle s_{a_1 b_2}^{++} \rangle = \langle s_{a_2 b_2}^{++} \rangle, \quad (\text{A18c})$$

$$\langle s_{a_2 a_1}^{+-} \rangle = \langle s_{a_1 a_2}^{+-} \rangle = \langle s_{b_2 b_1}^{-+} \rangle = \langle s_{b_1 b_2}^{-+} \rangle, \quad (\text{A18d})$$

$$\langle s_{b_1 b_1}^{+-} \rangle = \langle s_{b_2 b_2}^{+-} \rangle = \langle s_{a_1 a_1}^{-+} \rangle = \langle s_{a_2 a_2}^{-+} \rangle, \quad (\text{A18e})$$

$$\langle s_{a_1 b_1}^{--} \rangle = \langle s_{a_2 b_2}^{--} \rangle = \langle s_{b_1 a_1}^{++} \rangle = \langle s_{b_2 a_2}^{++} \rangle, \quad (\text{A18f})$$

$$\langle s_{a_2 b_1}^{--} \rangle = \langle s_{a_1 b_2}^{--} \rangle = \langle s_{b_2 a_1}^{++} \rangle = \langle s_{b_1 a_2}^{++} \rangle, \quad (\text{A18g})$$

and

$$\langle s_{b_2 b_1}^{+-} \rangle = \langle s_{b_1 b_2}^{-+} \rangle = \langle s_{a_2 a_1}^{-+} \rangle = \langle s_{a_1 a_2}^{-+} \rangle. \quad (\text{A18h})$$

The values of the spin correlation function can be obtained with the help of Eqs. (A4)–(A10) by using the symmetry shown in Eq. (A18).

\*Email address: govind@mail.nplindia.ernet.in

<sup>1</sup>P. W. Anderson, *The Theory of Superconductivity in High  $T_c$  Cuprates* (Princeton University Press, Princeton, NJ, 1997).

<sup>2</sup>B. Batlogg, *Physica C* **282–287**, 130 (1997).

<sup>3</sup>E. Dagatto, *Rev. Mod. Phys.* **66**, 763 (1994).

<sup>4</sup>J. Jaklic and P. Prelovsek, *Adv. Phys.* **49**, 1 (2000).

<sup>5</sup>Y. D. Chuang, A. D. Gromko, D. S. Dessau, Y. Aiura, Y. Yamaguchi, K. Oka, A. J. Arko, J. Joyce, H. Eisaki, S. I. Uchida, K.

- Nakamura, and Y. Ando, cond-mat/9904050 (unpublished).
- <sup>6</sup>T. Sato, T. Kamiyama, Y. Naitoh, T. Takahashi, I. Chong, T. Terashima, and M. Takano, Phys. Rev. B **63**, 132502 (2001).
- <sup>7</sup>T. Yoshida, X. J. Zhou, M. Nakamura, S. A. Kellar, E. D. Lu, A. Lanzara, Z. Hussain, A. Ino, T. Mizokawa, A. Fujimori, H. Eisaki, C. Kim, Z. X. Shen, T. Kakeshita, and S. Uchida, Phys. Rev. B **63**, 220501 (2001).
- <sup>8</sup>J. Mesot, M. Renderia, M. R. Norman, A. Kaminski, H. M. Fretwell, J. C. Campuzano, H. Ding, T. Takeuchi, T. Sato, T. Yokoya, T. Takahashi, I. Chong, T. Terashima, M. Takano, T. Mochiku, and K. Kadowaki, Phys. Rev. B **63**, 224516 (2001).
- <sup>9</sup>T. Sato, T. Kamiyama, T. Takahashi, J. Mesot, A. Kaminski, J. C. Campuzano, H. M. Fretwell, T. Takeuchi, H. Ding, I. Chong, T. Terashima, and M. Takano, Phys. Rev. B **64**, 054502 (2001).
- <sup>10</sup>A. Ino, C. Kim, M. Nakamura, T. Yosida, T. Mizokawa, Z. X. Shen, A. Fujimori, T. Kakeshita, H. Eisaki, and S. Uchida, Phys. Rev. B **62**, 4137 (2000).
- <sup>11</sup>P. Aebi, J. Osterwalder, P. Schwaller, L. Sclapbach, M. Shimoda, T. Mochiku, and K. Kadowaki, Phys. Rev. Lett. **72**, 2757 (1994).
- <sup>12</sup>H. M. Fretwell, A. Kaminski, J. Mesot, J. C. Campuzano, M. R. Norman, M. Renderia, T. Sato, R. Gatt, T. Takahashi, and K. Kadowaki, Phys. Rev. Lett. **84**, 4449 (2000).
- <sup>13</sup>M. S. Golden, S. V. Borisenko, S. Lenger, T. Pichler, C. Durr, M. Knupfer, J. Fink, G. Yang, S. Abell, G. Reichaedt, R. Muller, and C. Janowitz, Physica C **341–348**, 2099 (2000).
- <sup>14</sup>J. Mesot, M. Boehm, M. R. Norman, M. Renderia, N. Metoki, A. Kaminski, S. Rosenkranz, A. Hiess, H. M. Fretwell, J. C. Campuzano, and K. Kadowaki, cond-mat/0102339 (unpublished).
- <sup>15</sup>Y. D. Chuang, A. D. Gromko, A. Fedorov, D. S. Dessau, Y. Aiura, K. Oka, Y. Ando, H. Eisaki, and S. I. Uchida, cond-mat/0102386 (unpublished).
- <sup>16</sup>D. L. Feng, N. P. Armitage, D. H. Lu, A. Damascelli, J. P. Hu, P. Bogdanov, A. Lanzara, F. Ronning, K. M. Shen, H. Esaki, C. Kim, Z. X. Shen, J. J. Shimoyama, and K. Kishio, Phys. Rev. Lett. **86**, 5550 (2001).
- <sup>17</sup>A. A. Kordyuk, S. V. Borisenko, M. S. Golden, S. Legner, K. A. Nenkov, M. Knupfer, J. Fink, H. Berger, and L. Forro, Phys. Rev. B **66**, 014502 (2002).
- <sup>18</sup>Y. D. Chuang, A. D. Gromko, A. Fedorov, Y. Aiura, K. Oka, Y. Ando, and D. S. Dessau, cond-mat/0107002 (unpublished).
- <sup>19</sup>Z. X. Shen and J. R. Schrieffler, Phys. Rev. Lett. **78**, 1771 (1997).
- <sup>20</sup>D. L. Feng, A. Damascelli, K. M. Shen, N. Motoyama, D. H. Lu, H. Eisaki, K. Shimizu, J. I. Shimoyama, K. Kishio, N. Kaneko, M. Greven, G. D. Gu, X. J. Zho, C. Kim, F. Ronning, N. P. Armitage, and Z. X. Shen, cond-mat/0108186 (unpublished).
- <sup>21</sup>E. Dagotto, R. Joynt, A. Moreo, S. Bacci, and E. Gagliano, Phys. Rev. B **41**, 9049 (1990).
- <sup>22</sup>D. Poiblanc, T. Ziman, H. J. Schulz, and E. Dagatto, Phys. Rev. B **47**, 14 267 (1993).
- <sup>23</sup>A. Moreo, S. Hass, A. W. Sanwikand, and E. Dagatto, Phys. Rev. B **51**, 12 045 (1995).
- <sup>24</sup>M. Bononsegni and E. Monousakis, Phys. Rev. B **47**, 11 897 (1993).
- <sup>25</sup>N. Bulut, D. J. Scalapino, and S. R. White, Phys. Rev. B **50**, 7215 (1994).
- <sup>26</sup>R. Preuss, W. Hanke, C. Grober, and H. G. Evertz, Phys. Rev. Lett. **79**, 1122 (1997).
- <sup>27</sup>S. R. White, Phys. Rev. Lett. **69**, 2863 (1992).
- <sup>28</sup>X. Wang and T. Xiang, Phys. Rev. B **56**, 5061 (1997).
- <sup>29</sup>J. Jaklic and P. Prelovsek, Phys. Rev. Lett. **77**, 892 (1996).
- <sup>30</sup>J. Jaklic and P. Prelovsek, Phys. Rev. B **55**, R7307 (1997).
- <sup>31</sup>P. W. Anderson, Science **235**, 1196 (1987).
- <sup>32</sup>S. Chakarvarty, A. Sudbo, P. W. Anderson, and S. Strong, Science **261**, 337 (1993).
- <sup>33</sup>A. I. Liechtenstein, O. Gunnarsson, O. K. Anderson, and R. M. Martin, Phys. Rev. B **54**, 12 505 (1996); O. K. Anderson, A. I. Liechtenstein, O. Jopsen, and F. Paulsen, J. Phys. Chem. Solids **56**, 1573 (1995).
- <sup>34</sup>A. Pratap, Govind, and R. S. Tripathi, Phys. Rev. B **60**, 6775 (1999).
- <sup>35</sup>A. Pratap, R. Lal, Govind, and S. K. Joshi, Phys. Rev. B **64**, 224512 (2001).
- <sup>36</sup>P. A. Lee, *High-Temperature Superconductivity*, The Los Alamos Symposium—1989 Proceeding, editors K. S. Bedell, D. Coffey, D. E. Meltzer, D. Pines, and J. R. Schrieffer (Addison-Wesley, Redwood City, 1990), p. 96.
- <sup>37</sup>C. L. Kane, P. A. Lee, and N. Read, Phys. Rev. B **39**, 6880 (1989).
- <sup>38</sup>D. Arovav and A. Auerbach, Phys. Rev. B **38**, 316 (1998).
- <sup>39</sup>J. L. Richard and V. Yu. Yushankhai, Phys. Rev. B **47**, 1103 (1993); **50**, 12 927 (1994).
- <sup>40</sup>C. Kim, P. J. White, Z. X. Shen, T. Tohyama, Y. Shibata, S. Meakawa, B. O. Welles, Y. J. Kim, R. J. Birgeneau, and M. A. Kaster, Phys. Rev. Lett. **80**, 4245 (1998).
- <sup>41</sup>G. Baskaran, Z. Zou, and P. W. Anderson, Solid State Commun. **63**, 973 (1997).
- <sup>42</sup>Z. Wang, Y. Bang, and G. Kotliar, Phys. Rev. Lett. **67**, 2733 (1991).
- <sup>43</sup>B. Keimer, N. Belk, R. J. Birgeneau, A. Cassanho, C. Y. Chen, M. Greven, M. A. Kastner, A. Aharony, Y. Endoh, R. W. Erwin, and G. Shirane, Phys. Rev. B **46**, 14 034 (1992).
- <sup>44</sup>B. P. Stojkovic and D. Pines, Phys. Rev. B **56**, 11 931 (1997).
- <sup>45</sup>Ratan Lal, Solid State Commun. **115**, 359 (2000).
- <sup>46</sup>Ratan Lal, Physica C **340**, 71 (2000).
- <sup>47</sup>C. M. Verma, P. B. Littlewood, S. Schmitt-Rink, E. Abrahams, and A. E. Ruckenstein, Phys. Rev. Lett. **26**, 1996 (1989).
- <sup>48</sup>Z. Schlesinger, R. T. Collins, F. Holtzberz, C. Field, S. H. Blaton, U. Welp, G. W. Crabtree, Y. Fang, and J. Z. Liu, Phys. Rev. Lett. **65**, 801 (1990).
- <sup>49</sup>S. Uchida, Physica C **185–189**, 28 (1991).
- <sup>50</sup>A. V. Puchkov, D. N. Basov, and T. Timusk, J. Phys.: Condens. Matter **8**, 10 049 (1997), and references therein.